8-1-2015

Building a Better Infarct: Modulation of Collagen Cross-Linking to Increase Infarct Stiffness and Reduce Left Ventricular Dilation Post-Myocardial Infarction

Andrew P. Voorhees
University of Texas at San Antonio

Kristine Y. DeLeon-Pennell
San Antonio Cardiovascular Proteomics Center

Yonggang Ma
San Antonio Cardiovascular Proteomics Center

Ganesh V. Halade
San Antonio Cardiovascular Proteomics Center, ghalade@usf.edu

Andriy Yabluchanskiy
San Antonio Cardiovascular Proteomics Center

See next page for additional authors

HHS Public Access

Author manuscript

J Mol Cell Cardiol. Author manuscript; available in PMC 2016 August 01.

Published in final edited form as:

J Mol Cell Cardiol. 2015 August ; 85: 229–239. doi:10.1016/j.yjmcc.2015.06.006.

Building a Better Infarct: Modulation of Collagen Cross-linking to Increase Infarct Stiffness and Reduce Left Ventricular Dilation post-Myocardial Infarction

Andrew P. Voorhees, Ph.D.[1,2,3], **Kristine Y. DeLeon-Pennell, Ph.D.**[3,4], **Yonggang Ma, Ph.D.**[3,4], **Ganesh V. Halade, Ph.D.**[3,5], **Andriy Yabluchanskiy, Ph.D.**[3,4,6], **Rugmani Padmanabhan Iyer, Ph.D.**[3,4], **Elizabeth Flynn**[4], **Courtney A. Cates**[4], **Merry L. Lindsey, Ph.D.**[2,3,4,6], and **Hai-Chao Han, Ph.D.**[1,2,3]

[1]Department of Mechanical Engineering, The University of Texas at San Antonio

[2]Joint Biomedical Engineering Program, UTSA-UTHSCSA

[3]San Antonio Cardiovascular Proteomics Center

[4]Mississippi Center for Heart Research, Department of Physiology and Biophysics, University of Mississippi Medical Center

[5]Division of Cardiovascular Disease, Department of Medicine, The University of Alabama at Birmingham

[6]Research Service, G.V. (Sonny) Montgomery Veterans Affairs Medical Center

Abstract

Matrix metalloproteinase-9 (MMP-9) deletion attenuates collagen accumulation and dilation of the left ventricle (LV) post-myocardial infarction (MI); however the biomechanical mechanisms underlying the improved outcome are poorly understood.

The aim of this study was to determine the mechanisms whereby MMP-9 deletion alters collagen network composition and assembly in the LV post-MI to modulate the mechanical properties of myocardial scar tissue. Adult C57BL/6J wild-type (WT; n=88) and MMP-9 null (MMP-9$^{-/-}$; n=92) mice of both sexes underwent permanent coronary artery ligation and were compared to day 0 controls (n=42). At day 7 post-MI, WT LVs displayed a 3-fold increase in end-diastolic volume, while MMP-9$^{-/-}$ showed only a 2-fold increase ($p<0.05$). Biaxial mechanical testing revealed that MMP-9$^{-/-}$ infarcts were stiffer than WT infarcts, as indicated by a 1.3-fold reduction in predicted *in vivo* circumferential stretch ($p<0.05$). Paradoxically, MMP-9$^{-/-}$ infarcts had a 1.8-fold reduction in collagen deposition ($p<0.05$). This apparent contradiction was explained by a 3.1-fold increase

Corresponding Author: Hai-Chao Han, Ph.D., Department of Mechanical Engineering, The University of Texas at San Antonio, Biomedical Engineering Program, UTSA-UTHSCSA, 1 UTSA Circle, San Antonio, TX, 78249, Phone: (210) 458-4952, hchan@utsa.edu.

Disclosures

The authors declare no conflict of interest.

in lysyl oxidase ($p<0.05$) in MMP-$9^{-/-}$ infarcts, indicating that MMP-9 deletion increased collagen cross-linking activity. Furthermore, MMP-9 deletion led to a 3.0-fold increase in bone morphogenetic protein-1, the metalloproteinase that cleaves pro-collagen and pro-lysyl oxidase ($p<0.05$) and reduced fibronectin fragmentation by 49% ($p<0.05$) to enhance lysyl oxidase activity. We conclude that MMP-9 deletion increases infarct stiffness and prevents LV dilation by reducing collagen degradation and facilitating collagen assembly and cross-linking through preservation of the fibronectin network and activation of lysyl oxidase.

Keywords

Cardiac mechanics; collagen crosslinking; matrix metalloproteinase-9; lysyl oxidase; infarct stiffness; proteomics

1. Introduction

Myocardial infarction (MI) is a leading cause of death in the United States [1]. Post-MI, the left ventricle (LV) undergoes a dynamic cascade of remodeling events that result in increased LV size, decreased wall thickness, and reduced cardiac function [2]. LV dilation post-MI is the result of myocyte destruction and excessive degradation of the myocardial extracellular matrix (ECM) without adequate synthesis of new ECM components [3]. ECM remodeling is a key determinant of patient outcomes, as new ECM deposition in the infarct zone reduces infarct dilation and decreases the chance of cardiac rupture, while excessive ECM depositiProteinaseon can lead to stiffer scar tissue that hinders diastolic filling [4–6].

Myocardial scar tissue is mechanically a non-linear anisotropic material [3, 7]. While the properties of the normal myocardium are dominated by the structure and orientation of the myocytes, the properties of the infarct region are primarily governed by the network of newly deposited collagen fibers [3, 8]. Biaxial mechanical testing is the gold standard for testing planar anisotropic materials, making this method ideal for studying how variations in the properties of the collagen network alter scar mechanics in a mouse MI model [7, 9, 10]. Biomechanical analysis of infarct tissue, therefore, provides a critical understanding of the complex interactions between ECM structure, LV function, and patient outcome.

In order to vary the properties of the collagen network we utilized matrix metalloproteinase (MMP)-9 null (MMP-$9^{-/-}$) mice, a model that has been well studied [11, 12]. MMPs are a class of proteins responsible for proteolysis of ECM proteins, and MMP-9, amongst its myriad targets, degrades both collagen and fibronectin [13, 14]. Fragments of these proteins trigger inflammation and increase deposition of new ECM proteins including collagen I and III [15–17]. MMP-9 deletion has been shown to prevent LV dilation, lower collagen deposition, and increase angiogenesis in mice post-MI [12, 18]. Despite these findings, the exact mechanisms by which MMP-9 deletion prevents adverse remodeling remain unclear; and given the cleavage targets of MMP-9, this is an excellent model for examining how variations in the collagen network alter infarct biomechanics.

Since MMP-9 degrades both collagen and the fibronectin network upon which collagen is assembled, we hypothesized that MMP-9 deletion would alter infarct stiffness. An increase

in infarct stiffness could explain the reduction in LV dilation observed in MMP-9 null mice and could contribute to a reduction in LV remodeling through reduced myocardial wall stress. The aim of this study was to determine how MMP-9 deletion alters the mechanical properties of myocardial scar tissue and the composition and assembly of the collagen network post-MI.

2. Methods

2.1 Animals and Surgery

All animal procedures were performed based on the "Guide for the Care and Use of Laboratory Animals" and have been approved by the Institutional Animal Care and Use Committee at the University of Texas Health Science Center at San Antonio and University of Mississippi Medical Center. Adult (4–10 month old) C57BL/6J mice (WT; n=51 female and 59 male including day 0 controls), and MMP-9 null mice (MMP-9$^{-/-}$; n=62 female and 50 male including day 0 controls) were used in this study. MI was induced through permanent ligation of the left coronary artery following a well-established method [19, 20]. In summary, mice were anesthetized with 1–2% isoflurane in 100% oxygen, intubated, and placed on a standard rodent ventilator. An incision was made between the 3rd and 4th intercostal space, and a rib spreader was used to allow visualization of the heart. An 8-0 suture was used to ligate the left coronary artery at a location approximately 1–2 mm distal to the left atrium, and MI was confirmed by LV blanching and ST segment elevation on the electrocardiogram. Immediately before or after surgery, buprenorphine (0.1 mg/kg) was administered intraperitoneally to reduce pain. Animals were sacrificed at 1, 3, 5, 7, or 28 days post-MI. We have previously published survival, echocardiography, and collagen density analysis results for WT vs MMP-9$^{-/-}$ at day 28 post-MI [21]. To avoid unnecessary duplication of animal use, those results have been integrated into the current study. All data have been re-analyzed in accordance with the methods used for this study. Day 0, no MI, served as controls. In an effort to minimize the number of animals, samples were shared across studies leading to varying sample sizes across groups.

2.2 Echocardiography

Echocardiography was performed using either a Vevo 770 system or a Vevo 2100 small animal imaging system (Visual Sonics). Imaging occurred serially at day 0 before surgery and at days 1, 3, 5, and 7 post-MI or up to the sacrifice time. Day 28 images, taken from a previous study, were also analyzed but were not measured serially. All images were taken with mice anesthetized with 1–2% isoflurane in an oxygen mix. Images were taken in both long and short axes views in both M-mode and B-mode. LV volumes and ejection fraction (EF, %) were calculated from long axis views, while LV dimensions were calculated from short axis views. All calculations were determined by averaging the values of three consecutive cardiac cycles. Dimensions for each mouse were normalized to its baseline image to evaluate relative changes.

Speckle tracking analysis was done using the VevoStrain analysis program (Visual Sonics). Longitudinal deformation was measured from long-axis views. Tracking data was exported to Matlab for further analysis. Stretch of the base region and mid-ventricle region was

calculated from an average of three cardiac cycles. Measurements were made at end-diastole, the end of isovolumic contraction, end-systole, and the end of isovolumic relaxation.

2.3 Tissue Collection

Prior to sacrifice, mice were anesthetized with 2–5% isoflurane. Cardioplegic solution was used to arrest the heart in diastole to ensure isolation of passive non-contracted tissue. The LV was separated from the right ventricle and sliced into apex, middle, and base sections. The pieces were stained with 1% 2, 3, 5-triphenyltetrazolum chloride and photographed in order to determine the percentage of infarct area to total LV area. The mid wall ring was sectioned into the infarct wall and septal wall and used for mechanical testing. The ratio of lung weight to tibia length was measured as an index for edema.

2.4 Mechanical Testing

Mechanical testing was performed using a Biotester-5000 biaxial test system (Cellscale) following a previously described method [22]. The stresses and corresponding strains were fit to a four parameter Fung-type model where the strain energy density was calculated as:

$$W=\frac{1}{2}c(e^{Q}-1), \quad Q=b_1{E_\theta}^2+b_2{E_z}^2+2b_4E_\theta E_z \quad (1)$$

to yield the Cauchy stress expressed as

$$\begin{aligned}\sigma_\theta&=(1+2E_\theta)(b_1E_\theta+b_4E_z)ce^{Q}\\ \sigma_z&=(1+2E_z)(b_2E_z+b_4E_\theta)ce^{Q}\end{aligned} \quad (2)$$

where c, b_1, b_2, and b_4 are the four material constants and E_θ and E_z are the circumferential and longitudinal Green strains [22, 23]. Fitted material properties for each individual sample were calculated as well as group averaged material properties. Tissue stiffness was quantified as the slope of the Cauchy stress-stretch ratio curve between 5 and 15% equibiaxial stretch. *In vivo* wall stresses were estimated using the Law of Laplace, with the average wall thickness and dimension at end diastole determined from echocardiography for each sample. An end-diastolic pressure of 10 mm Hg was chosen based on our previously collected experimental data for the healthy mouse LV [12]. The estimated stresses and the fitted material properties for each sample were used to back-calculate the expected *in vivo* deformation.

2.5 Collagen Histology

Histological analysis using picrosirius red (PSR) staining was used to examine collagen density and alignment. Collagen density was measured from ring sections of the LV taken from the midcavity wall. Slides for collagen alignment were taken from the samples used for mechanical testing and processed following a previously described method [22]. PSR stained LV rings were imaged with a brightfield microscope at 40x magnification with three representative images taken in the infarct region and two images taken in the remote region. Slides for collagen alignment were imaged at 10x magnification with three images taken

near the middle of the infarct region for each slide and one additional image of the edge of the specimen taken so as to denote the circumferential direction. An in-house program written in Matlab was used to measure collagen density and alignment from PSR stained sections, which has been previously described [22].

2.6 Immunoblotting

LV specimens were separated into infarct and remote regions. For each time point, samples from the infarct region of n=8 mice (4 female and 4 male) were analyzed. Total protein was extracted following a previously described method [11].

LV protein expression levels were quantified by immunoblotting using antibodies for Collagen I (Cedarlane cl50141ap; 1:3000), Collagen III (Cedarlane cl50341ap-1; 1:1000), lysyl oxidase (Novus nb110-41568; 1:2000), fibronectin (Millipore AB1954; 1:1000) and bone morphogenetic protein-1 (Abcam ab38953; 1:5000). Antibodies for collagen I, collagen III, and lysyl oxidase recognize both pro-form and active form proteins. Total protein (10 μg) was separated on 4–12% Criterion™ XT Bis-Tris gels (Bio-Rad), transferred to a nitrocellulose membrane (Bio-Rad), and stained with MemCode™ Reversible Protein Stain Kit (Thermo Scientific) to verify protein concentration and loading accuracy. After blocking with 5% nonfat milk (Bio-Rad), the membrane was incubated with primary antibody, secondary antibody (Vector Laboratories, PI-1000, 1:5000), and detected with ECL Prime Western Blotting Detection Substrate (Amersham). Protein levels were quantified by densitometry using the IQ-TL image analysis software (GE Healthcare, Waukesha, WI). The densitometry of the entire lane of the total protein stained membrane was used for individual lane loading normalization. The relative expression for each immunoblot was calculated as the densitometry of the protein of interest divided by the densitometry of the entire lane of the total protein stained membrane. For each protein of interest, blots were run in triplicate.

2.7 Collagen Cross-Linking

An enzyme-linked immunosorbent assay (ELISA) was used to quantify the amounts of hydroxylysyl pyridinoline (ABIN809022) and lysyl pyridinoline (ABIN773391) following a previously described method [24].

2.8 Real Time RT^2-PCR

Gene expression of MMP-2 was determined using a Quantitative Real Time RT^2-PCR gene array for MMPs and tissue inhibitors of metalloproteinases (Qiagen PAMM-013A) following our previously method [11].

2.9 Statistical Analysis

All data are presented as mean ± SEM. Analysis was performed using one-way ANOVA followed by a Student Newman Keuls post-hoc test for multiple comparisons, a t-test for comparisons between two groups, or a Mann-Whitney U test. A post-hoc one sample t-test was used to determine if echocardiography data normalized to d0 controls was significantly different from the control. Analysis was conducted using Graphpad Prism (Graphpad).

3. Results

3.1 MMP-9 Deletion Reduced All-Cause Mortality and Prevented LV dilation

As previously reported [11], WT survival at day 7 post MI was 55%, while MMP-9 deletion significantly improved the survival rate to 82% ($p<0.05$). The 28 day survival has also been previously reported for these mice as 38% for WT and 67% for MMP-$9^{-/-}$ ($p<0.05$) [21].

Serial echocardiography examination of the progression of LV dilation showed that MI produced a significant increase in both end-diastolic volume and end-systolic volume, in both WT and MMP-$9^{-/-}$ mice, which was observed at all time points ($p<0.05$). We found that the relative change in end-diastolic volume was significantly less in the MMP-$9^{-/-}$ group compared to WT at both day 5 and day 7 post-MI ($p<0.05$, Fig. 1A). LV dilation at day 28 post-MI was similar to dilation at day 7 post-MI. The change in end-systolic volume was also significantly reduced with MMP-9 deletion ($p<0.05$, Fig. 1B). Ejection fraction, and end-diastolic wall thickness were significantly impaired by MI at all time points ($p<0.05$), and no differences were observed between the WT and MMP-$9^{-/-}$ groups (Fig 1C–D) indicating similar levels of systolic dysfunction. No differences were observed in the percentage of infarct area between WT and MMP-$9^{-/-}$ at day 7 post-MI ($p=0.90$), indicating that differences were not due to initial ischemia injury differences. In total, we confirmed from echocardiography that LV dilation was significantly reduced in the MMP-$9^{-/-}$ group, with intergroup differences peaking at 7 days post-MI, similar to what we have reported in previous studies [12, 18].

3.2 MMP-9 Deletion Increases Infarct Stiffness

Since post-MI LV dilation was attenuated in the absence of MMP-9, we used biaxial mechanical testing to determine if the differences in LV dilation were due to differences in the mechanical properties of the infarct tissue. The Fung-type constitutive equation fit the stress-strain measurements very nicely, with an average R^2 correlation coefficient for the individual material constants of 0.975 and a minimum value of 0.857. The high R^2 values indicate that the Fung-type strain energy density equation is an excellent choice for modeling the mechanical behavior of both healthy and infracted myocardial tissue. The group averaged material constants for the infarct tissues had increased exponential constants (b_1, b_2, and b_4) compared to the healthy tissue indicating increased anisotropic, exponential stress-strain behavior (Table 1). The infarct tissue demonstrated a highly exponential stress-strain curve, consistent with the infarct being more collagenous than the normal LV (Fig. 2A–B).

The circumferential stiffness was significantly increased in both the WT and MMP-$9^{-/-}$ groups compared to their respective healthy controls ($p<0.05$, Fig. 2C) indicating that the infarct tissue was stiffer in the circumferential direction as compared to healthy tissue. However, the longitudinal stiffness was only significantly increased for the MMP-$9^{-/-}$ infarct group compared to the healthy MMP-$9^{-/-}$ baseline group ($p<0.05$, Fig. 2D), indicating that MMP-9 deletion results in infarct tissue with increased longitudinal stiffness.

To determine whether the differences in mechanical properties between the groups altered the diastolic function of the infarct tissue, the amount of *in vivo* diastolic stretch was

estimated based on the Law of Laplace. Circumferential stretch in both the day 7 post-MI groups was significantly increased compared to baseline ($p<0.05$, Fig. 2E). Further, the estimated *in vivo* circumferential stretch was significantly lower in the MMP-$9^{-/-}$ group as compared to the WT. The predicted longitudinal stretch was significantly increased in both day 7 post-MI groups ($p<0.05$, Fig. 2F), however no differences were seen between the WT and MMP-$9^{-/-}$ groups. As a whole, the mechanical testing findings of increased longitudinal stiffness for a fixed deformation and reduced circumferential stretch under fixed pressure suggest that infarct tissue from the MMP-$9^{-/-}$ mice is stiffer than the infarct tissue from the WT mice. No significant difference in the edema index was found between the groups ($p=0.87$) ruling out edema as a potential source of the mechanical differences.

3.3 Increased Infarct Stiffness Improves the Mechanics of the Remote Non-infarcted Myocardium

Speckle tracking echocardiography was used to examine the *in vivo* deformation of the myocardial tissue. Longitudinal stretch was measured in both the mid-wall and basal regions of the LV between end-diastole and the end of isovolumic contraction at day 7 post-MI in order to study infarct bulging. No significant difference in longitudinal stretch of the mid-wall region was seen between the WT (1.40±0.24%) and the MMP-$9^{-/-}$ group (0.59±0.39%; $p=0.097$; Fig. 3A). There was, however, a significant reduction in negative longitudinal stretch, or contraction, of the basal region at the end of isovolumic contraction for the MMP-$9^{-/-}$ group as compared to WT ($p<0.05$; Fig. 3B). A reduction in contraction of the remote basal region during isovolumic contraction is consistent with an increase in infarct stiffness due to a reduction of infarct bulging.

In vivo stretch was also measured between the end of isovolumic relaxation and end-diastole in an effort to correlate our *in vivo* and *ex vivo* mechanical measurements. End-diastolic longitudinal stretch of the mid-ventricle region was not correlated to the *ex vivo* circumferential stress at 20% equibiaxial stress (Fig. 3C). However, increased circumferential stress was correlated with increased longitudinal stretch of the basal region ($p<0.05$; Fig. 3D). This indicates that increased stiffness of the infarct region promotes stretch of the healthy tissue regions rather than stretch of the infarct region during diastolic filling which could aid cardiac function through the Frank-Starling mechanism. No significant correlation was seen between *in vivo* longitudinal strains in the two regions and the *ex vivo* longitudinal stress under 20% equibiaxial stretch.

3.4 MMP-9 Deletion Reduces Collagen Deposition

Since collagen is considered to be the primary determinant of infarct mechanics at day 7 post-MI [3], we focused on quantifying collagen network properties. Our PSR analysis revealed that collagen density was significantly increased in the infarct area in both groups at day 7 post-MI as compared to baseline ($p<0.05$, Fig. 4A,B). Furthermore, MMP-9 deletion significantly reduced collagen density in the infarct area at day 7 (12.2±2.7%) as compared to WT (21.3±5.4%; $p<0.05$). At 28 days post-MI, collagen levels were significantly elevated from baseline, but no significant differences were found between the groups. Analysis of the remote area also revealed significantly elevated collagen density at day 7 post-MI compared to baseline ($p<0.05$, Fig. 3A,B), but no significant difference

between genotypes. Representative images from each time point appear in the online supplement (Fig.S1)

The distribution of collagen fibers in either the WT or MMP-9$^{-/-}$ group at day 7 post-MI was not significantly different from a uniform distribution (WT, p=0.23; MMP-9$^{-/-}$, p=0.19; Fig. 4C). The mean alignment of the fibers tended to rotate through the thickness of the tissue similar to the rotation pattern of myocytes in healthy tissue, such that fibers near the epicardial surface were aligned at an angle of roughly −50 degrees to the circumferential direction and fibers at the endocardial surface were aligned at an angle of roughly 50 degrees. No differences were seen in either the mean angle of the fibers at the epicardial surface (p=0.71) or in the amount of rotation through the thickness of the tissue (p=0.09). The collagen alignment data suggests that differences in infarct mechanical properties are not due to a difference in collagen organization.

Since PSR cannot distinguish between the various isoforms of collagen, immunoblotting was conducted for both collagen I and collagen III (Fig. 5 A,B). The amount of collagen I was increased at day 7 in the WT group compared to baseline, and reduced in the MMP-9$^{-/-}$ group as compared to the WT ($p<0.05$, Fig. 5C). A significant increase in collagen I fragments, as compared to baseline, was found at day 5 and 7 post-MI in the WT group, but not in the MMP-9$^{-/-}$ group ($p<0.05$, Fig 5D) consistent with reduced protease activity in the MMP-9$^{-/-}$ infarct.

The expression of pro-collagen III was significantly reduced from baseline at day 3, 5, and 7 in the WT group and at all days in the MMP-9$^{-/-}$ group as compared to baseline, but no differences were observed between the two genotypes ($p<0.05$, Fig. 5E). Analysis of collagen III revealed significantly elevated levels of collagen III at day 5 and 7 compared to baseline in WT and at day 7 in the MMP-9$^{-/-}$ groups ($p<0.05$, Fig. 5F). The collagen I to collagen III ratio was 1.8±0.45 for WT at day 7 post-MI, and was 0.34±0.52 for the MMP-9$^{-/-}$ at day 7 post-MI (p=0.13). In total, the collagen immunoblotting data indicates that the differences in collagen density observed from PSR staining were primarily due to differences in collagen I levels.

3.5 MMP-9 Deletion Facilitates Collagen Assembly and Crosslinking

Collagen is known to be the primary determinant of infarct mechanics during the fibrotic phase of remodeling [3]. Given the observation that MMP-9$^{-/-}$ mice exhibited signs of increased tissue stiffness with reduced collagen density, we hypothesized that a difference in the quality of the collagen in the scar tissue exists. Immunoblotting results showed that active lysyl oxidase, a catalyst for collagen fibril assembly and crosslinking, was significantly elevated in the MMP-9$^{-/-}$ mice compared to both the baseline MMP-9$^{-/-}$ group and the day 7 WT post-MI group ($p<0.05$, Fig. 6A,B). Interestingly, the inactive forms of lysyl oxidase were significantly reduced in both groups, as compared to baseline at every time point ($p<0.05$, Fig 6A,C). Inactive lysyl oxidase was also significantly reduced in the MMP-9$^{-/-}$ group compared to WT at day 7 ($p<0.05$). These results indicate improved activation of lysyl oxidase in the MMP-9$^{-/-}$. ELISA analysis did not reveal any statistical differences in the amount of hydroxylysyl pyridionline crosslinks (Fig. 6D, p=0.30) or lysyl pyridinoline crosslinks (Fig. 6E, p=0.26) at day 7 post-MI. The lack of significance was not

surprising, given the fact that the MMP-9$^{-/-}$ infarct contains significantly less collagen I (Fig. 5C). Therefore, a similar level of total cross-linking represents a greater number of crosslinks per collagen fiber in the MMP-9$^{-/-}$ infarct.

Additionally, bone morphogenetic protein-1 a metalloproteinase responsible for cleaving the propeptide from lysyl oxidase as well as from collagens I and III, was significantly reduced at day 3 and 5 post-MI in the WT group and at day 3 in the MMP-9$^{-/-}$ group as compared to baseline ($p<0.05$, Fig 6F,H). A significant increase in bone morphogenetic protein-1 was found in the MMP-9$^{-/-}$ group compared to the WT group at day 7 post-MI ($p<0.05$). This data suggests that the increase in lysyl oxidase activation in the MMP-9$^{-/-}$ group is at least partially due to the increase in bone morphogenetic protein-1. Further, the increase in bone morphogenetic protein-1 may lead to an increase in the rate at which pro-collagen I is cleaved into its active form.

Fibronectin serves as a scaffold for collagen fiber formation and has been shown to facilitate the activation of lysyl oxidase by bone morphogenetic protein-1 [25]. Fibronectin is also a cleavage target of MMP-9 [14]. Our results showed that the fibronectin fragmentation ratio was significantly elevated at days 5 and 7 post-MI in the WT group and day 5 post-MI in the MMP-9$^{-/-}$ group compared to baseline, and there was a significant reduction in fibronectin fragmentation at day 7 due to MMP-9 deletion ($p<0.05$, Fig. 6G,I).

The gene expression of MMP-2, the other major gelatinase, was quantified using RT^2-PCR. No significant difference was found between the WT and MMP-9$^{-/-}$ group at day 7 post-MI ($p=0.58$), indicating that MMP-2 did not compensate for the loss of MMP-9, which agrees with the decreases we observed in both collagen and fibronectin fragmentation. As a whole, our data indicate that MMP-9 deletion preserves fibronectin integrity and allows for the activity of lysyl oxidase and bone morphogenetic protein-1 which facilitate collagen fiber formation and cross-linking.

4. Discussion

This study revealed that MMP-9 deletion modifies the mechanical properties of infarct tissue by altering the structure and assembly of the collagen network post-MI. We found that MMP-9 deletion increased infarct stiffness, surprisingly not through increased collagen content but rather through increased collagen cross-linking activity and reduced collagen degradation. In fact, MMP-9 deletion actually facilitated collagen assembly by reducing fibronectin degradation and increasing lysyl oxidase and bone morphogenetic protein-1 activities. Increased stiffness of the infarct region promoted stretch of the remote non-infarcted basal region of the LV during diastolic filling and limited stretch of the basal region during isovolumic contraction consistent with reduced infarct bulging. Our results identify a potential mechanism by which MMP-9 deletion prevents LV dilation, further establishing MMP-9 as a candidate selective therapeutic target (Fig. 7).

Understanding the mechanical properties of infarct tissue is important for understanding the mechanisms of post-MI outcomes. Infarct tissue that is too compliant can lead to LV dilation and even cardiac rupture, while tissue that is too stiff can lead to diastolic heart failure [3]. The mechanical strength and stiffness of collagen derive from proper fiber assembly and

cross-linking [26]. A mutation in the collagen α2(I) gene in mice prevents proper assembly of collagen I and results in increased LV dilation and rupture post-MI [27]. The formation of the covalent crosslinks that stabilize the collagen fibers is primarily catalyzed by lysyl oxidase [28]. Lysyl oxidase itself is activated by the protease bone morphogenetic protein-1, which also cleaves the C-terminal peptide from pro-collagen [29]. Our study demonstrates that MMP-9 deletion significantly increases the amount of activated lysyl oxidase in the infarcted myocardium at day 7 post-MI and significantly reduces the amount of inactive lysyl oxidase as compared to WT. The proteolytic activation of lysyl oxidase by bone morphogenetic protein-1 is facilitated by fibronectin which serves as a scaffold for the assembly of collagen fibers [25]. Fibronectin is a substrate for MMP-9 cleavage [17], and we observed decreased fibronectin fragmentation in the MMP-$9^{-/-}$ mice. The decreased turnover of fibronectin likely improves the activation of lysyl oxidase by bone morphogenetic protein-1 and in turn the assembly of collagen fibers in the MMP-$9^{-/-}$ mice as described in Fig. 7.

Based on both this study and previous findings, MMP-9 deletion reduces the overall fibrotic response through multiple mechanisms [12, 18]. While we have presented an argument here for enhanced collagen assembly and reduced collagen turnover leading to reduced infarct dilation, there is still work to be done in determining the mechanisms that lead to reduced fibrosis. Cardiac lysyl oxidase and bone morphogenetic protein-1 expression have been tied to transforming growth factor-β signaling, a driver of cardiac fibrosis [30]. The fibrotic response normally operates as a negative feedback system with increased fibrosis occurring in response to increased ECM breakdown.[31] Thus fibrosis can be reduced by limiting the amount of ECM turnover. ECM fragments, such as fibronectin or collagen fragments have been shown to bind cell surface receptors and trigger increased fibrotic responses [17, 32]. We showed that the deletion of MMP-9 limits the formation of fibronectin fragments, which could explain the decreased fibrosis. Alterations in tissue stresses have also been shown to modulate collagen synthesis, with increased levels of stress sparking increased collagen deposition [33]. Based on the law of Laplace, increased LV volume and decreased wall thickness should lead to increased LV stresses which would explain the enhanced fibrosis post MI. Another possibility lies in increased angiogenesis. MMP-9 deletion has been shown to facilitate blood vessel formation which could reduce hypoxic stress levels, further reduce fibrosis and preserve the border zone regions [12, 34]. Likely, it is a combination of these mechanisms that leads to the reduced fibrosis.

The relationship between the myocardial scar quality and its mechanical properties during the acute stages post-MI is challenging to define, in part due to rapid shifts in the cell populations involved and in the molecular composition of the left ventricle in response to the ischemic insult. Therefore, the findings reported in the current study provide a view that is focused on the early stage of the maturation phase. Future studies that incorporate the later mechanical changes will give better insight into the long-term scar quality. These studies could help determine if the more mature WT infarct with its high collagen content becomes stiffer than the MMP-$9^{-/-}$ infarct. It would be important to know if MMP-9 deletion both prevents dilation at early time points and prevents diastolic dysfunction at later time points through a reduction in fibrosis.

Of note, this study found few functional differences between the WT and MMP-9$^{-/-}$ groups at day 1 and 3 post-MI. This time phase aligns with the inflammatory period of the wound healing process [3]. MMP-9 is widely expressed by neutrophils and macrophages and has been reported to play a large role in cleaving the basement membrane to allow neutrophil invasion [35, 36]. There are differences in the inflammatory response between the WT and MMP-9$^{-/-}$ mice that may set the stage for the functional differences that develop during the onset of fibrosis at days 5 and 7 post-MI [11, 12]. Given the decrease in rupture rates for the MMP-9$^{-/-}$ mice noted in past studies, further examination of tissue mechanics during the inflammatory period is merited [37]. Treatments that aim to increase infarct stiffness throughout the inflammatory process may reduce early LV dilation and infarct expansion into the border zones through reduced mechanical stress.

Cross-linking is only one of the determinants of collagen mechanics. Properties such collagen fiber diameter and the ratio of collagen I to III all contribute to the mechanical behavior at the tissue level [4, 6]. Thick, stiff collagen fibers are typically the result of proper collagen assembly and maturation, which are largely regulated through the actions of lysyl oxidase and fibronectin. Efforts to associate the ratio of collagen I to collagen III with increased infarct stiffness have been numerous, however the meaning of the measurement can be difficult to interpret as it neglects the importance of total collagen [6]. In this study, we did not find a statistically significant difference in the ratio of collagen I to collagen III. Future work should include the use of polarized light microscopy to more directly quantify fiber diameter, collagen I to III ratios, and collagen crimp.

One limitation of this study is that we have only explored one avenue of lysyl oxidase regulation, activation by bone morphogenetic protein-1. Lysyl oxidase is known to be regulated by multiple factors that are differentially regulated in the remodeling infarct including hypoxia inducible factor-1α, advanced glycation end products, transforming growth factor-β, and reactive oxygen species [28]. Further investigation is needed to determine how these factors may interact with both MMP-9 and lysyl oxidase.

The results of this study suggest several avenues of potential therapeutic strategies beyond simply inhibiting MMP-9. Directly increasing the stiffness of the infarct region is one avenue. This concept has been tested by injecting polymer based hydrogels into the infarct site to prevent dilation [38]. Other techniques such as attaching patches of support material to the exterior of the LV have also been investigated with promising results [39, 40]. A more pharmacological approach could be in delivering activated lysyl oxidase or bone morphogenetic protein-1 to the infarct site. The future of treatment for MI likely rests in regenerative medicine, however the post-MI fibrotic process regulates stem cell differentiation [41], and the stiffness of the ECM is a controller of angiogenesis [42]. Technologies that aim to limit the initial dilation of the myocardium and control ECM stiffness hold great value as complimentary therapies to regenerative approaches.

In conclusion, we demonstrated that MMP-9 deletion facilitates collagen I fiber formation during the early stages of fibrosis resulting in a stiffer infarct region that limits LV dilation and prevents further adverse remodeling post-MI.

Supplementary Material

Refer to Web version on PubMed Central for supplementary material.

Acknowledgments

This work was supported by the National Heart, Lung, and Blood Institute [HHSN 268201000036C (N01-HV-00244)] for the San Antonio Cardiovascular Proteomics Center. It was also partially supported by the American Heart Association (AHA) [POST14350034 to KYD-P and 14POST18770012 to RPI], the Biomedical Laboratory Research and Development Service of the Veterans Affairs Office of Research and Development Award [5I01BX000505 to MLL], and the National Institutes of Health [K99-AT006704 to GVH, R01HL075360 to MLL, R01HL095852 to HCH], and by HL051971, and GM104357 from the NIH.

References

1. Roger VL, Go AS, Lloyd-Jones DM, Adams RJ, Berry JD, Brown TM, et al. Executive Summary: Heart Disease and Stroke Statistics-2011 Update A Report From the American Heart Association. Circulation. 2011; 123:459–63.
2. Cohn JN, Ferrari R, Sharpe N. Cardiac Remodeling- Concepts and Clinical Implications: A Consensus Paper From an International Forum on Cardiac Remodeling. J Am Coll Cardiol. 2000; 35:569–82. [PubMed: 10716457]
3. Holmes JW, Borg TK, Covell JW. Structure and mechanics of healing myocardial infarcts. Annu Rev Biomed Eng. 2005; 7:223–53. [PubMed: 16004571]
4. Voorhees A, Han H-C. A model to determine the effect of collagen fiber alignment on heart function post myocardial infarction. Theoretical Biology and Medical Modelling. 2014; 11:6. [PubMed: 24456675]
5. Bogen DK, Rabinowitz SA, Needleman A, McMahon TA, Abelmann WH. An analysis of the mechanical disadvantage of myocardial infarction in the canine left ventricle. Circulation Research. 1980; 47:728–41. [PubMed: 7418131]
6. Fomovsky GM, Thomopoulos S, Holmes JW. Contribution of extracellular matrix to the mechanical properties of the heart. Journal of Molecular and Cellular Cardiology. 2010; 48:490–6. [PubMed: 19686759]
7. Gupta KB, Ratcliffe MB, Fallert MA, Edmunds LH Jr, Bogen DK. Changes in passive mechanical stiffness of myocardial tissue with aneurysm formation. Circulation. 1994; 89:2315–26. [PubMed: 8181158]
8. Omens JH, Miller TR, Covell JW. Relationship between passive tissue strain and collagen uncoiling during healing of infarcted myocardium. Cardiovascular Research. 1997; 33:351–8. [PubMed: 9074699]
9. Fomovsky GM, Holmes JW. Evolution of scar structure, mechanics, and ventricular function after myocardial infarction in the rat. American Journal of Physiology-Heart and Circulatory Physiology. 2010; 298:H221–H8. [PubMed: 19897714]
10. Wang B, Tedder M, Perez C, Wang G, Jongh Curry A, To F, et al. Structural and biomechanical characterizations of porcine myocardial extracellular matrix. J Mater Sci: Mater Med. 2012; 23:1835–47. [PubMed: 22584822]
11. DeLeon-Pennell KY, de Castro Brás LE, Iyer RP, Bratton DR, Jin Y-F, Ripplinger CM, et al. P. gingivalis lipopolysaccharide intensifies inflammation post-myocardial infarction through matrix metalloproteinase-9. Journal of Molecular and Cellular Cardiology. 2014; 76:218–26. [PubMed: 25240641]
12. Lindsey ML, Escobar GP, Dobrucki LW, Goshorn DK, Bouges S, Mingoia JT, et al. Matrix metalloproteinase-9 gene deletion facilitates angiogenesis after myocardial infarction. Am J Physiol Heart Circ Physiol. 2006; 290:H232–9. [PubMed: 16126817]
13. Lindsey ML, Weintraub ST, Lange RA. Using Extracellular Matrix Proteomics to Understand Left Ventricular Remodeling. Circulation: Cardiovascular Genetics. 2012; 5:o1–o7. [PubMed: 22337931]

14. Zamilpa R, Lopez EF, Chiao YA, Dai Q, Escobar GP, Hakala K, et al. Proteomic analysis identifies in vivo candidate matrix metalloproteinase-9 substrates in the left ventricle post-myocardial infarction. Proteomics. 2010; 10:2214–23. [PubMed: 20354994]
15. Adair-Kirk TL, Senior RM. Fragments of extracellular matrix as mediators of inflammation. The International Journal of Biochemistry & Cell Biology. 2008; 40:1101–10. [PubMed: 18243041]
16. Gardi C, Calzoni P, Marcolongo P, Cavarra E, Vanni L, Lungarella G. Collagen breakdown products and lung collagen metabolism: an in vitro study on fibroblast cultures. Thorax. 1994; 49:312–8. [PubMed: 8202899]
17. Marom B, Rahat MA, Lahat N, Weiss-Cerem L, Kinarty A, Bitterman H. Native and fragmented fibronectin oppositely modulate monocyte secretion of MMP-9. Journal of Leukocyte Biology. 2007; 81:1466–76. [PubMed: 17327485]
18. Ducharme A, Frantz S, Aikawa M, Rabkin E, Lindsey M, Rohde LE, et al. Targeted deletion of matrix metalloproteinase-9 attenuates left ventricular enlargement and collagen accumulation after experimental myocardial infarction. J Clin Invest. 2000; 106:55–62. [PubMed: 10880048]
19. Salto-Tellez M, Yung Lim S, El Oakley RM, Tang TPL, Almsherqi ZAM, Lim S-K. Myocardial infarction in the C57BL/6J mouse: A quantifiable and highly reproducible experimental model. Cardiovascular Pathology. 2004; 13:91–7. [PubMed: 15033158]
20. Zamilpa R, Kanakia R, Cigarroa J, Dai Q, Escobar GP, Martinez H, et al. CC chemokine receptor 5 deletion impairs macrophage activation and induces adverse remodeling following myocardial infarction. American Journal of Physiology - Heart and Circulatory Physiology. 2011; 300:H1418–H26. [PubMed: 21297029]
21. Ramirez TA, Iyer RP, Ghasemi O, Lopez EF, Levin DB, Zhang J, et al. Aliskiren and valsartan mediate left ventricular remodeling post-myocardial infarction in mice through MMP-9 effects. J Mol Cell Cardiol. 2014; 72:326–35. [PubMed: 24768766]
22. Grimes KM, Voorhees A, Chiao YA, Han HC, Lindsey ML, Buffenstein R. Cardiac function of the naked mole-rat: ecophysiological responses to working underground. Am J Physiol Heart Circ Physiol. 2014; 306:H730–7. [PubMed: 24363308]
23. Tong P, Fung Y-C. The stress-strain relationship for the skin. Journal of Biomechanics. 1976; 9:649–57. [PubMed: 965417]
24. Ma Y, Halade GV, Zhang J, Ramirez TA, Levin D, Voorhees AP, et al. Matrix Metalloproteinase-28 Deletion Exacerbates Cardiac Dysfunction and Rupture Following Myocardial Infarction in Mice by Inhibiting M2 Macrophage Activation. Circ Res. 2012; 20:20.
25. Fogelgren B, Polgár N, Szauter KM, Újfaludi Z, Laczkó R, Fong KSK, et al. Cellular Fibronectin Binds to Lysyl Oxidase with High Affinity and Is Critical for Its Proteolytic Activation. Journal of Biological Chemistry. 2005; 280:24690–7. [PubMed: 15843371]
26. Uzel SGM, Buehler MJ. Molecular structure, mechanical behavior and failure mechanism of the C-terminal cross-link domain in type I collagen. Journal of the Mechanical Behavior of Biomedical Materials. 2011; 4:153–61. [PubMed: 21262493]
27. Hofmann U, Bonz A, Frantz S, Hu K, Waller C, Roemer K, et al. A Collagen α2(I)Mutation Impairs Healing after Experimental Myocardial Infarction. The American Journal of Pathology. 2012; 180:113–22. [PubMed: 22067913]
28. López B, González A, Hermida N, Valencia F, de Teresa E, Díez J. Role of lysyl oxidase in myocardial fibrosis: from basic science to clinical aspects. American Journal of Physiology - Heart and Circulatory Physiology. 2010; 299:H1–H9. [PubMed: 20472764]
29. Panchenko MV, Stetler-Stevenson WG, Trubetskoy OV, Gacheru SN, Kagan HM. Metalloproteinase Activity Secreted by Fibrogenic Cells in the Processing of Prolysyl Oxidase: Potential Role of procollagen C-Proteinase. Journal of Biological Chemistry. 1996; 271:7113–9. [PubMed: 8636146]
30. Voloshenyuk TG, Landesman ES, Khoutorova E, Hart AD, Gardner JD. Induction of cardiac fibroblast lysyl oxidase by TGF-β1 requires PI3K/Akt, Smad3, and MAPK signaling. Cytokine. 2011; 55:90–7. [PubMed: 21498085]
31. Rouillard AD, Holmes JW. Coupled agent-based and finite-element models for predicting scar structure following myocardial infarction. Prog Biophys Mol Biol. 2014

32. Okamura Y, Watari M, Jerud ES, Young DW, Ishizaka ST, Rose J, et al. The Extra Domain A of Fibronectin Activates Toll-like Receptor 4. Journal of Biological Chemistry. 2001; 276:10229–33. [PubMed: 11150311]
33. Rouillard AD, Holmes JW. Mechanical regulation of fibroblast migration and collagen remodeling in healing myocardial infarcts. The Journal of Physiology. 2012
34. Yabluchanskiy A, Ma Y, Chiao YA, Lopez EF, Voorhees AP, Toba H, et al. Cardiac aging is initiated by matrix metalloproteinase-9-mediated endothelial dysfunction. Am J Physiol Heart Circ Physiol. 2014; 306:H1398–407. [PubMed: 24658018]
35. Lambert JM, Lopez EF, Lindsey ML. Macrophage roles following myocardial infarction. International Journal of Cardiology. 2008; 130:147–58. [PubMed: 18656272]
36. Bradley LM, Douglass MF, Chatterjee D, Akira S, Baaten BJG. Matrix Metalloprotease 9 Mediates Neutrophil Migration into the Airways in Response to Influenza Virus-Induced Toll-Like Receptor Signaling. PLoS Pathog. 2012; 8:e1002641. [PubMed: 22496659]
37. Heymans S, Luttun A, Nuyens D, Theilmeier G, Creemers E, Moons L, et al. Inhibition of plasminogen activators or matrix metalloproteinases prevents cardiac rupture but impairs therapeutic angiogenesis and causes cardiac failure. Nat Med. 1999; 5:1135–42. [PubMed: 10502816]
38. Gorman R, Jackson B, Burdick J, Gorman J. Infarct Restraint to Limit Adverse Ventricular Remodeling. Journal of Cardiovascular Translational Research. 2011; 4:73–81. [PubMed: 21161462]
39. Blom A, Pilla J, Gorman R, Gorman J, Mukherjee R, Spinale F, et al. Infarct Size Reduction and Attenuation of Global Left Ventricular Remodeling with the CorCap^{TM} Cardiac Support Device Following Acute Myocardial Infarction in Sheep. Heart Failure Reviews. 2005; 10:125–39. [PubMed: 16258720]
40. Fomovsky GM, Clark SA, Parker KM, Ailawadi G, Holmes JW. Anisotropic Reinforcement of Acute Anteroapical Infarcts Improves Pump Function / Clinical Perspective. Circulation: Heart Failure. 2012; 5:515–22. [PubMed: 22665716]
41. Sullivan KE, Quinn KP, Tang KM, Georgakoudi I, Black LD 3rd. Extracellular matrix remodeling following myocardial infarction influences the therapeutic potential of mesenchymal stem cells. Stem Cell Res Ther. 2014; 5:14. [PubMed: 24460869]
42. Underwood CJ, Edgar LT, Hoying JB, Weiss JA. Cell-generated traction forces and the resulting matrix deformation modulate microvascular alignment and growth during angiogenesis. Am J Physiol Heart Circ Physiol. 2014; 307:H152–64. [PubMed: 24816262]

Highlights

- MMP-9 deletion reduced left ventricular (LV) dilation post-myocardial infarction.
- MMP-9 deletion increased scar stiffness but reduced collagen deposition.
- MMP-9 deletion enhanced lysyl oxidase activation, increasing collagen crosslinking.
- Early collagen crosslinking prevents excessive LV dilation via improved mechanics.

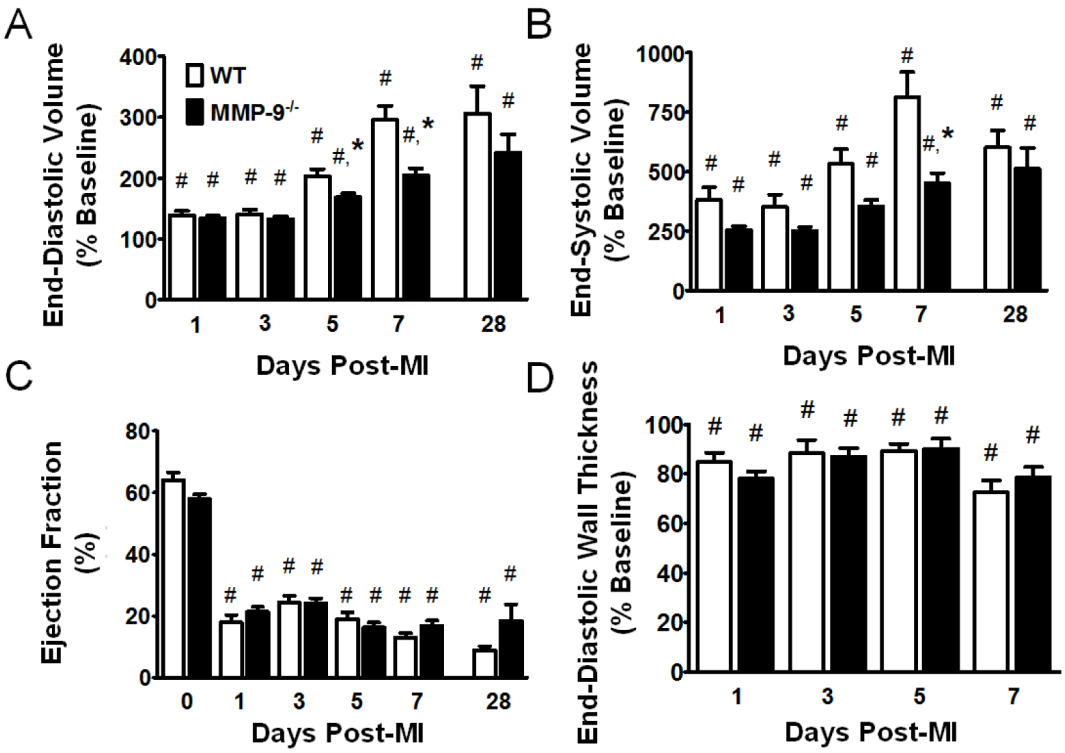

Figure 1. Matrix metalloproteinase-9 (MMP-9) deletion reduces dilation of the left ventricle (LV) at days 5 and 7 post-myocardial infarction (MI)

A. MI resulted in increased end-diastolic volume in both groups at all time points ($p<0.05$). The change in end diastolic volume from baseline was significantly decreased in MMP-$9^{-/-}$ mice at day 5 and 7 post-MI. **B.** MI also resulted in increased end-systolic volume in both groups at all time points ($p<0.05$). The change in end-systolic volume was significantly decreased in MMP-$9^{-/-}$ mice at day 7 post-MI. **C.** MI significantly reduced ejection fraction at all time points in both groups, and no significant differences were observed between the groups. **D.** MI led to a significant reduction in end-diastolic wall thickness in both groups, at each time-point ($p<0.05$), and no differences were observed between the WT and MMP-$9^{-/-}$ groups. Note that day 0–7 data is presented from serial images taken on the same mice, while day 28 data is from a different set of mice. (n=15–32 per group for day 0–7 groups and n=6 per group for day 28; #$p<0.05$ vs. corresponding baseline group, *$p<0.05$ vs. WT at corresponding day)

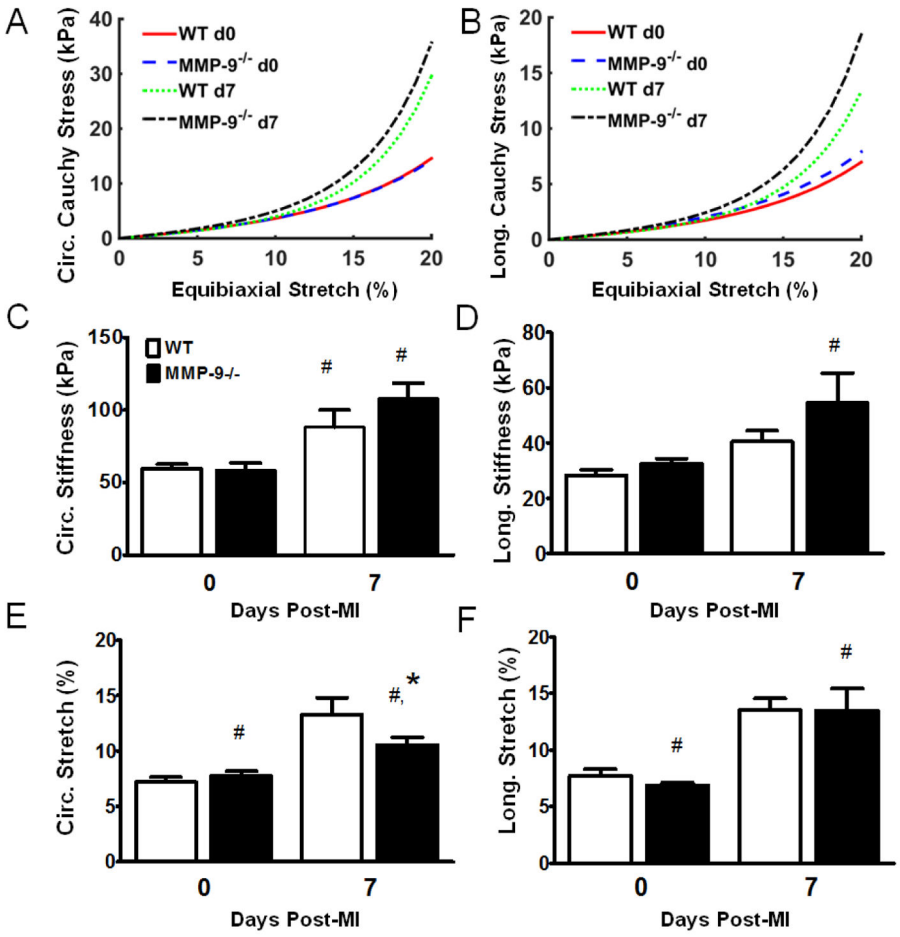

Figure 2. Matrix metalloproteinase-9 (MMP-9) deletion increases infarct stiffness and reduces infarct stretching at day 7 post-myocardial infarction (MI)

A. The mean circumferential Cauchy stress vs. equibiaxial stretch curve indicates a trend towards increased circumferential stiffness in the MMP-9$^{-/-}$ day 7 post-MI left ventricle (LV). **B.** The mean longitudinal Cauchy stress vs. equibiaxial stretch curve indicates a trend towards increased longitudinal stiffness in the MMP-9$^{-/-}$ day 7 post-MI LV. **C.** The circumferential stiffness between 5% and 15% equibiaxial stretch was significantly increased in both groups compared to the baseline controls, indicating increased stiffness due to MI. **D.** The longitudinal stiffness was significantly increased in only the MMP-9$^{-/-}$ group as compared to the baseline group. **E.** The predicted circumferential *in vivo* stretch of the infarct was significantly increased in both groups as compared to baseline. However, MMP-9$^{-/-}$ day 7 post-MI LV showed significantly reduced stretch compared to WT day 7 post-MI LV. **F.** The predicted longitudinal *in vivo* stretch of the infarct was significantly increased in both groups as compared to baseline. (n=12 per group; #p<0.05 vs. corresponding baseline group, *p<0.05 vs. WT at corresponding day)

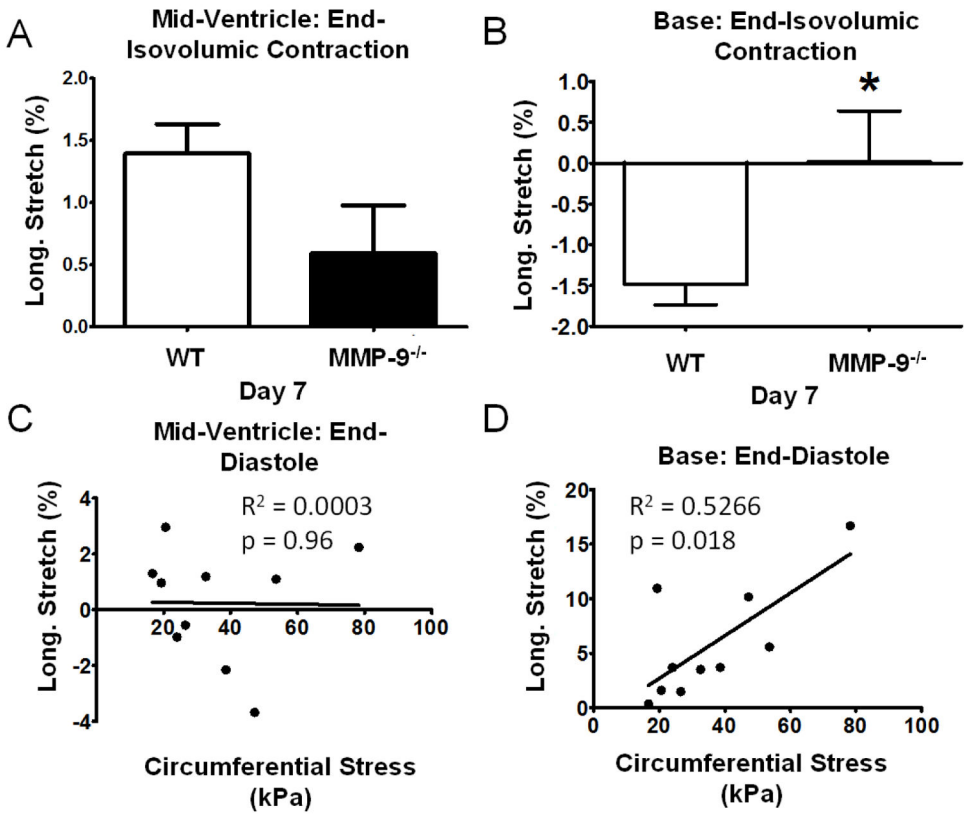

Figure 3. Increased infarct stiffness prevents stretch of the non-infarcted remote myocardium during isovolumic contraction and promotes stretch during diastolic filling

A. Longitudinal stretch of the mid-ventricle portion of the myocardial wall during isovolumic contraction, as determined from speckle-tracking echocardiography, was not different between the wildtype (WT) and matrix metalloproteinase-9 null (MMP-$9^{-/-}$) groups (n = 12–17 per group; p=0.097). **B.** Negative longitudinal stretch of the basal portion of the myocardial wall during isovolumic contraction was significantly reduced (n = 12–17 per group; $p<0.05$). **C.** Longitudinal stretch in the mid-ventricle was not correlated to increased circumferential stress under 20% equibiaxial stress as determined from biaxial mechanical testing (n=10). **D.** Longitudinal stretch was correlated to increased circumferential stress indicating that increased infarct stiffness enhances the stretch of the remote myocardium during diastole (n=10; $p<0.05$).

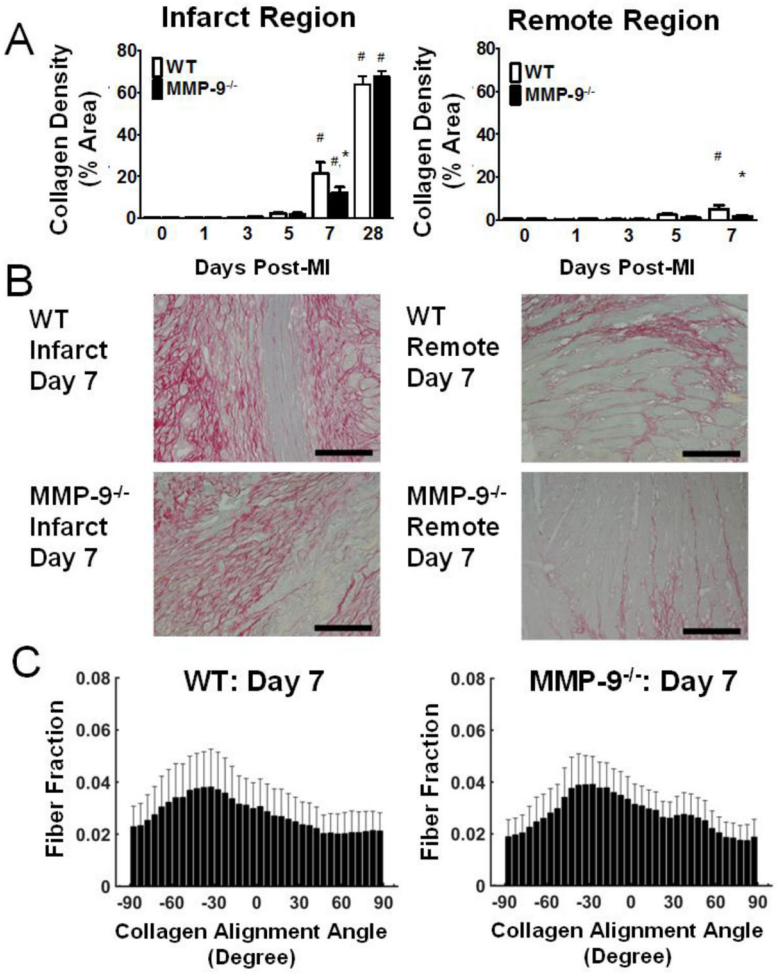

Figure 4. Matrix metalloproteinase-9 (MMP-9) deletion reduces collagen content at day 7 post-myocardial infarction (MI) but does not change the alignment of the collagen network

A. Picrosirius red (PSR) revealed significantly elevated levels of collagen in the infarct region at day 7 and day 28 post-MI (left). Collagen deposition was blunted by MMP-9 deletion at day 7. PSR staining also revealed increased collagen deposition in the remote region at day 7 as compared to baseline for WT (right, n=7–18 per group). **B.** Representative PSR stained images from WT and MMP-$9^{-/-}$ infarct (left) and remote (right) regions at day 7. **C.** Both WT (left) and MMP-$9^{-/-}$ (right) mice showed no significant alignment of collagen fibers (n=12 per group; p=0.23 for WT and p=0.19 for MMP-$9^{-/-}$). The lack of alignment is due to the fact that the newly deposited collagen fibers have a rotating orientation through the thickness of the wall following the pattern of myocyte alignment. This result indicates that the increased stiffness of the MMP-$9^{-/-}$ infarct is not due to changes in collagen alignment. (#p<0.05 vs. corresponding baseline group, *p<0.05 vs. WT at corresponding day)

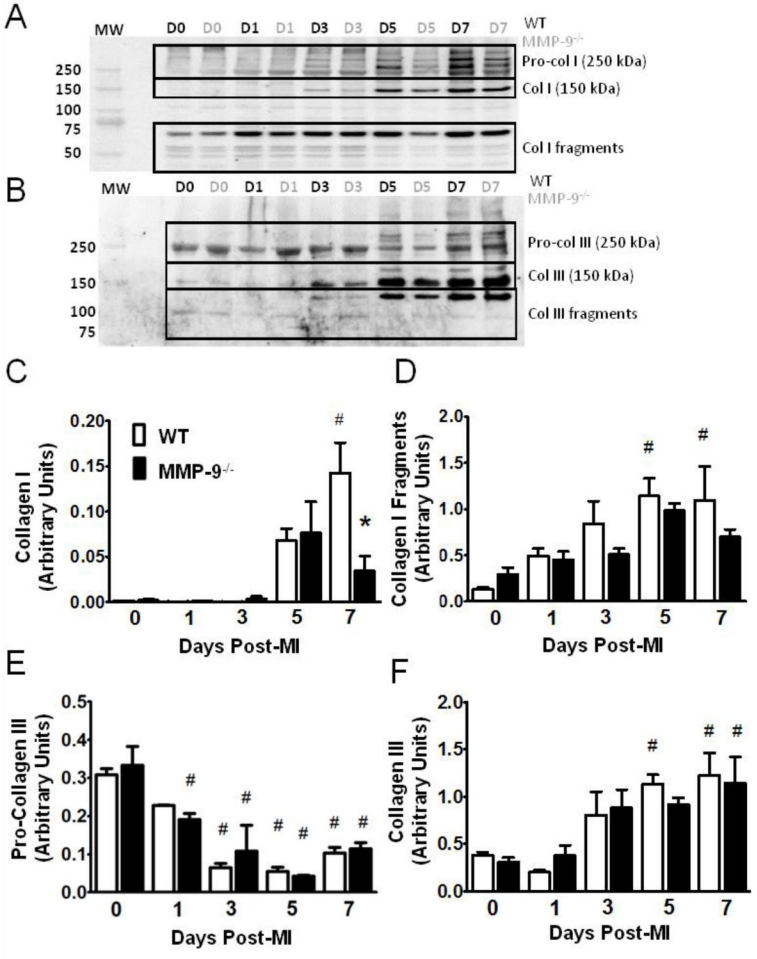

Figure 5. Matrix metalloproteinase-9 (MMP-9) deletion limits collagen I expression but not collagen III post-myocardial infarction (MI)

A–**B.** Immunoblot for Collagens I and III, showing pro-collagen, active collagen, and collagen fragments (D = day, MW = molecular weight). **C.** Significantly elevated levels of collagen I were found at day 7 in the WT group compared to baseline and the MMP-9$^{-/-}$ day 7 group. **D.** Significantly elevated levels of collagen I fragments were found in the WT group at day 5 and 7 post-MI, but no differences were seen in the MMP-9$^{-/-}$ group. **E.** Immunobloting revealed a significant decrease in the amount of pro-collagen III at day 3, 5, and 7 post-MI in the WT group and at day 1, 3, 5, and 7 post-MI in the MMP-9$^{-/-}$ group compared to baseline. **F.** A significant increase in collagen III was noted at day 5 and 7 post-MI in WT and at d7 in the MMP-9$^{-/-}$ group compared to respective baseline values. (n=8 per group; #p<0.05 vs. corresponding baseline group, *p<0.05 vs. WT at corresponding day)

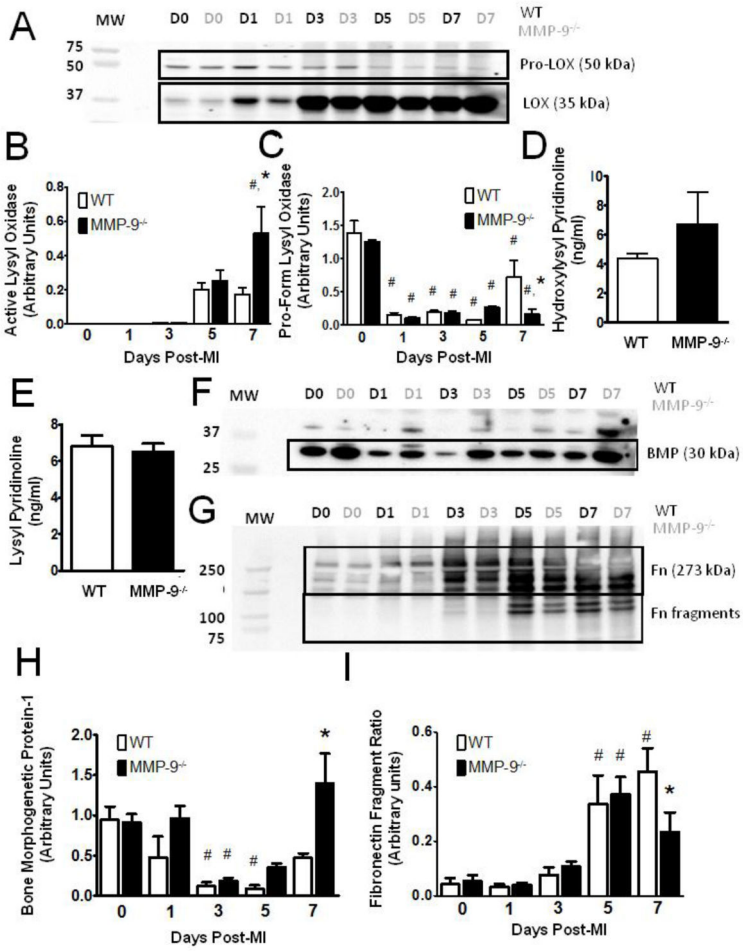

Figure 6. Matrix metalloproteinase-9 (MMP-9) deletion promotes collagen fibril formation and crosslinking

A. Immunoblot for lysyl oxidase (LOX) showing both inactive and active forms. (D = day, MW = molecular weight) **B.** Immunoblotting revealed significantly elevated levels of active LOX in the MMP-9$^{-/-}$ group as compared to both the baseline MMP-9$^{-/-}$ group and the WT day 7 MI group. **C.** The pro-form of LOX was significantly decreased from baseline in all MI groups, but the reduction was attenuated in the absence of MMP-9. **D–E.** Neither hydroxylysyl pyridinoline or lysyl pyrridinoline content was significantly different between the two groups at day 7 post-MI **F–G.** Immunoblots for bone morphogenetic protein-1 (BMP) and fibronectin (Fn), respectively. **H.** Expression of bone morphogenetic protein-1 was significantly reduced from baseline at day 3 and 5 post-MI in WT and at day 3 post-MI in MMP-9$^{-/-}$. Bone morphogenetic protein-1 expression was significantly elevated in the MMP-9$^{-/-}$ group at day 7 compared to WT. **H.** The ratio of the amounts of 120 and 80 kDa fibronectin fragments to the amount of 273 kDa full-length fibronectin revealed significantly elevated fragmentation of fibronectin at day 5 and 7 in the WT group and at day 5 in the MMP-9$^{-/-}$ group. The fragmentation ratio was significantly reduced in the MMP-9$^{-/-}$ group as compared to WT at day 7. (n=8 per group; #p<0.05 vs. corresponding baseline group, *p<0.05 vs. WT at corresponding day)

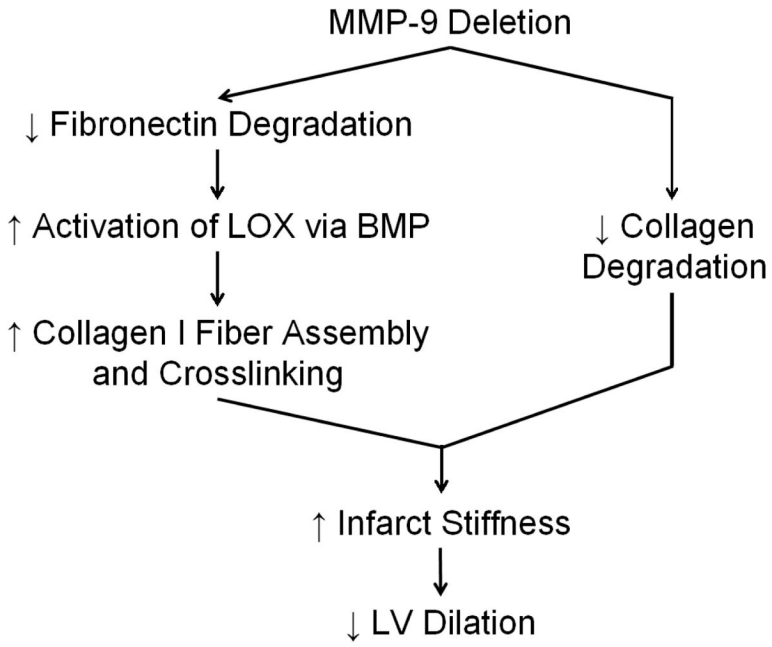

Figure 7. Potential Mechanism of Action for Decreased Dilation of the Left Ventricle (LV) in Matrix Metalloproteinase-9 Null (MMP-9$^{-/-}$) Mice Post-Myocardial Infarction (MI)

MMP-9 deletion preserves fibronectin structure, facilitating the activation of lysyl oxidase by bone-morphogenetic protein-1. Lysyl oxidase catalyzes the formation of collagen I cross-links thereby increasing the stiffness of the collagen fibers and the stiffness of the infarct tissue. Further, MMP-9 reduces collagen degradation, which also preserves tissue stiffness. Increased tissue stiffness reduces the stretching of the infarct region and the stresses in the border zones which reduces LV dilation.

Table 1

Fitted Material Constants from the Biaxial Test Data (see Equation 2)

Group	c (kPa)	b_1	b_2	b_4
WT Day 0	1.53	7.97	4.03	0.17
WT Day 7	0.57	19.52	8.60	0.44
MMP-9$^{-/-}$ Day 0	1.64	7.51	4.08	0.18
MMP-9$^{-/-}$ Day 7	0.70	19.06	9.68	0.34